32nd URSI GASS, Montreal, 19-26 August 2017

Truncation of Near- and Far-Fields in Directivity Estimation

Maryam Razmhosseini, Rodney G. Vaughan
Sierra Wireless Communications Laboratory, School of Engineering Science
Simon Fraser University, Burnaby, B.C., Canada, V5C 1S6

Abstract

The directivity and gain are the most challenging of the antenna parameters to measure accurately. Near-field (NF) techniques are now the preferred approach to direct far-field pattern estimation. The accuracy is of critical importance but it remains difficult to tie-down. This paper presents, from a user's viewpoint, experimental results of the effect of *truncation* of the field support and of the far-field (called *windowing*), on the estimated directivity. We use a professional-grade commercial measurement system with planar and cylindrical near-field samplers (NSI-200 V-5x5) to test a typical Ku-band 1.2 meter (~ 40 wavelengths) reflector antenna. Increasing the near-field truncation from the low energy part of the heat map acts to increase the directivity as expected, but as the truncation impinges more on the higher energy zone of the heat map, the directivity decreases. This experiment demonstrates that the choices of truncation and windowing for an optimal directivity estimate require further research.

1. Introduction

Near-field measurement techniques are described as fundamental solutions to the construction of precise and accurate test ranges for antenna far-field measurements [1]. Their development was motivated by the inherent difficulties of using far-field ranges. By the 1970s, pioneering work on NF pattern measurement at the US National Bureau of Standards in Boulder, CO., lead to a belief that NF measurements were likely more accurate than far-field approaches. Much analysis on the accuracy, and several pattern-measurement companies grew from this work. But the level of accuracy still attracts interest, partly due to the escalating accuracy claims of competing pattern-measurement system companies. These claims can be difficult to verify, with the biting constraint on gain accuracy, for example, sometimes being the accuracy of a calibration antenna or the probe antenna. The question then arises as to the accuracy of the measurement of the calibration antenna pattern, and so on. For the same antenna-under-test (AUT), different professional-grade NF pattern measurement systems can yield gains that differ by considerably more than the claimed accuracy of each system. How does a user choose from such results?

A basic step in developing near-field measurements is to identify and minimize the error sources. It is assumed that the computation (integration, transformation, interpolation, etc.) introduces negligible error. One approach for checking would be a parametric study of forward and backward transforms and record any error. (We have not done this.)

The physical location accuracy of the antennas' position and orientation, are widely regarded as minor compared to other error sources. This is because a system's robotics can be configured to cater for a given upper frequency, and the physical location and alignment accuracy of the antennas can be ascertained by laser techniques.

Any measurement is fundamentally limited by the signal-to-noise ratio (SNR) of its samples, but with the high dynamic ranges and available powers of modern microwave systems, this is also not currently regarded as the biting constraint on overall pattern measurement accuracy. However, we can demonstrate how the finite SNR can create problems when many parts of the NF measurement are very low SNR. An excess of low SNR in the heat map (can be reduced by truncation, see below) can add error to the far-field pattern, rather than act to help the measurement. A more signal-theoretic approach, such as using SNR-based weightings for undertaking the estimation step can help this problem.

The sampling spacing plays a role of course, with the measurement time being essentially proportional to the number of spatial samples. For a full directional spectrum of plane-wave fields, the sampling theorem suggests a spacing of closer than a half wavelength is required. A finite spectrum can reduce this spacing, - for example, according to the broadside array-spacing requirements (with standard notation and the usual assumptions),

$$d_{min} = \frac{\lambda_0}{1+\sin\theta_{max}} \ . \qquad (1)$$

But for NF measurements, the sampling aperture can be close to the AUT, and so the sampling density needs to cater for source region fields. There is scarce analytical information on this requirement, but the computational electromagnetics community often plumb for a tenth to a twentieth of a wavelength for numerical studies. Such a small spacing would make a typical NF measurement inconveniently slow, and in fact few commercial systems have the capability of such closely spaced sampling because of the large size of the measurement data. Our experiments have shown that the far-field patterns from otherwise-identical measurement configurations indeed depend on the sampling density even when the spacing is less than 0.3 of a wavelength.

Multipath propagation is also a stumbling block for the accuracy of both far-field and near-field measurements. In a NF chamber, the multipath within the chamber depends

on the patterns of the antennas. Different calibration antennas with different patterns will have different multipath degradation so the antenna substitution method appear to be vulnerable to this source of error. Direct reflections between the probe and the AUT are more obvious but are more manageable in the signal processing.

A fundamental source of error relates to being unable to measure the entire NF, and this is the subject of the rest of this paper. Spherical scanners can, in principle, sample all of the radiation aperture around an AUT. Cylindrical scanning ignores the end-caps of the cylinder as part of the aperture. Problems occur for "fat" cylindrical shapes where the end caps are significantly illuminated. Spherical, and to a lesser extent, cylindrical robotics, are expensive for deploying high positional accuracy. The simplicity of 2D cartesian robotics in a planar scan offers better positioning accuracy for a given cost. Planar scanning inherently has truncation of an AUT's full spherical aperture, and so its use is restricted to medium (and higher) gain antennas, where the NF illuminates the aperture and the illumination being assumed low everywhere else. *Truncation error* is the term used for the impact of using an incomplete NF aperture. For a directive pattern, which is of course the usual subject of a planar NF measurement, truncation of the lower intensity fields region acts to *increase* the estimate of the directivity owing to the shortfall in the captured total energy, e.g., [2]. The effect can be seen from the far-field directivity equation, in which the denominator is the total radiated energy and then assuming that this is the same as the total energy sampled in the NF. (In fact, the NFs also include reactive power so this assumption must be applied with care.) But an increasing truncation also cuts into the aperture size and so at some stage, increasing truncation must act to *decrease* the far-field directivity. Treating this tradeoff is still the subject of new research. For example, a new method published in 2006 [3] claims to eliminate the truncation error by utilizing the movement of the probe along an axis perpendicular to the scanning surface in order to recover the field in the part of an aperture external to the actual scanning area. In 2014, a truncation study [4] assessed the impact of the theta-direction truncation in a spherical near-field antenna test system. It demonstrates how the truncation has minor impact on the azimuth far-field and significant effect on the elevation far-field pattern.

Below, we present new experimental results to demonstrate the size of the truncation on antenna directivity in planar and cylindrical scanning systems. Our NF measurement system (NSI-200V-5x5) uses two directivity calculations which yield slightly different values. This helpful feature allows the user to assess the choices.

2. Directivity Calculation

The first choice is the classical (maximum) directivity,

$$D(\theta,\varphi) = \frac{|E_\theta(\theta,\varphi)|^2 + \left|E_\varphi(\theta,\varphi)\right|^2}{\frac{1}{4\pi}\oiint (|E_{tot}(\theta,\varphi)|^2)\sin\theta\, d\theta\, d\varphi} \tag{2}$$

where $|E_{tot}(\theta,\varphi)|^2 = |E_\theta(\theta,\varphi)|^2 + \left|E_\varphi(\theta,\varphi)\right|^2$, and unless otherwise specified, the *directivity* refers to the maximum *D*. The directivity is the sum of the polarized directivities, which can be written

$$D(\theta,\varphi) = D_\theta(\theta,\varphi) + D_\phi(\theta,\varphi) \tag{3}$$

and so the directivity is greater than the co-polar directivity, independent of the pattern shape of any non-zero cross-polar pattern. Calculation of each co-polar directivity requires the two scalar pattern measurements.

We can also have a scalar pattern directivity, such as

$$D_\theta^{(\theta)}(\theta_{max},\varphi_{max}) = \frac{|E_\theta(\theta_{max},\varphi_{max})|^2}{\frac{1}{4\pi}\oiint_{4\pi}(|E_\theta(\theta,\varphi)|^2)\sin\theta\, d\theta\, d\varphi}. \tag{4}$$

This scalar form can also be used in acoustics where the pressure or particle velocity would be used instead of the *E* or *H* far-fields. There appears to be no standard terminology for these various directivities, although the term "partial directivity" crops up with differing (or missing) definitions. For a system user, varying terminology such as this - which is ubiquitous - offers confusion.

The second form of directivity uses a windowed (called *filtered* in [6]) form of the calculated far-field pattern, where the outer directions of the pattern – those away from the main lobe – are set to zero in the style of a window in signal processing, and it is given by

$$\begin{aligned} &D_W(\theta,\varphi) \\ &= \frac{|E_\theta(\theta,\varphi)|^2 + \left|E_\varphi(\theta,\varphi)\right|^2}{\frac{1}{4\pi}\oiint_{4\pi} W_{(\theta,\varphi)}(\Delta\theta,\Delta\varphi)(|E_{tot}(\theta,\varphi)|^2)\sin\theta\, d\theta\, d\varphi} \\ &= \frac{|E_\theta(\theta,\varphi)|^2 + \left|E_\varphi(\theta,\varphi)\right|^2}{\frac{1}{4\pi}\int_{\Delta\theta}\int_{\Delta\varphi}(|E_{tot}(\theta,\varphi)|^2)\sin\theta\, d\theta\, d\varphi} \end{aligned} \tag{5}$$

This equation is our interpretation of how the windowed directivity is calculated in NSI's software and it is not provided in NSI documents. So our interpretation is that the full sphere of far-field pattern is calculated before the windowing calculation is taken. This is different to calculating only the windowed zone of the far-field first, and then calculating the directivity, with a possible associated scaling change of the far-field values (Parseval's theorem), including the value of the numerator. The window action is to capture the high energy directions, and set all the rest of the far-field pattern to zero. The omission of the finite radiated power outside the window directions (*cf.*, filter "stop band") means that $D > D_W$.

For convenience, the same window is used for both polarizations. For a directive pattern, the main lobe is typically in one of the polarizations, and the cross-polar pattern has a minimum in the same direction. So this windowing may have different, and even opposite, effects for the co- and cross-polar scalar directivities.

The support size of the window which is called the "valid far-field" region. For our NSI system [6], the describing formula appears to be from Yaghjian's analysis [7]. For a planar scanning system, the relationship between the

"maximum valid far-field angle" and the NF planar aperture, or scan size, is shown in Figure 1 [6].

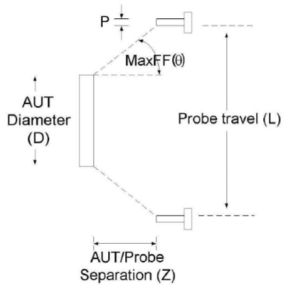

Figure 1. Relationship of max far-field angle and scan size in planar measurement [6].

This "maximum valid far-field angle" is from [6]

$$L = D + P + 2Z \tan\theta \tag{6}$$

where Z is the probe-to-AUT separation, L is the probe travel distance, D and P are the AUT and the probe diameter respectively.

For the cylindrical case, the near-field probe travel requirements and the relationship between the scan size and the maximum valid far-field is depicted in Figure 2 [6],

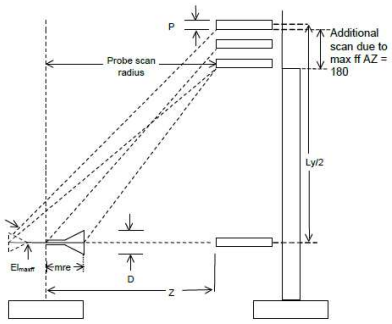

Figure 2. Relationship of max far-field angle and scan size in cylindrical measurement [6].

and the maximum valid far-field azimuth and elevation angle are related by [6]

$$L_y = D + P + 2\left(Z - mre\cos Az_{\max ff}\right)\tan El_{\max ff} \tag{7}$$

where L_y is the y-axis scan size, mre is the maximal radial extent, $Az_{\max ff}$ and $El_{\max ff}$ are the azimuth and the elevation maximum far-field angles respectively. For the far-fields outside of the window, the error is in the same order of magnitude as the far-field estimate [7] and this situation is referred to as a lack of confidence in the far-field pattern estimation outside the window support. It is tempting to consider that the difference between the two directivities relates to the accuracy of the directivity estimate from the NSI system. But such a conclusion is not fully supported and needs further research. In the example measurements below, the planar "maximum valid far-field angle" is 6 degrees and 5 degrees for θ and ϕ directions respectively, and for the cylindrical system, 180 degrees and 3 degrees respectively.

3. Measurement Setup

Figure 3 shows the AUT used in these measurements. It is a 1.2 meter Ku VSAT reflector fed by an offset linearly polarized horn. In this set-up, the probe locus comes within a couple of wavelengths of the horn but is well-spaced from the rest of the antenna. The probe is an NSI WR75 open ended waveguide that covers the frequency range of 10GHz to 15GHz. The probe includes a backplane which is absorber-covered, so the probe antenna structure is very lossy. Both planar and cylindrical scanning systems were deployed in the same set-up here.

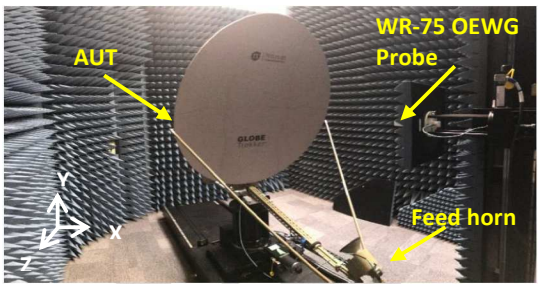

Figure 3. The AUT (1.2 m reflector) measured in NSI-200V-5x5 system deployed for planar and cylindrical NF scans.

4. Measurement Results

Figure 4 shows, for the cylindrical measurement, how the standard directivity and the windowed directivity differ. The maximum difference is about half a dB.

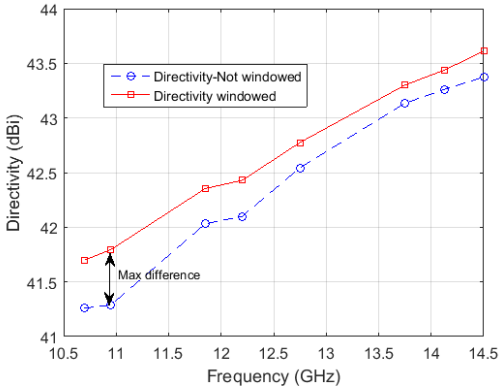

Figure 4. Azimuth-windowed (at 180 degrees) directivity and standard (unwindowed) directivity calculated from a cylindrical NF measurement.

Figure 5 shows the near-field intensity, or heat map, for the cylindrical aperture. The high intensity fields in front of

the reflector appear to be "well captured" in the ordinate with the truncation located at about -30dB relative to the maximum power. In azimuth, the backward directions indicate a near-field intensity of about -50dB relative to the maxima in the forward direction. The manufacturer's recommendation is to sample all areas that are within -30 dB (and preferably -40dB or more) from the peak NF value, to ensure accurate measurement. Figure 6 shows the far-field radiation patterns in azimuth before and after the azimuth truncation at $\phi=\pm 30^{o}$. The corresponding directivities, as well as those from a planar aperture measurement, are shown in Figure 7.

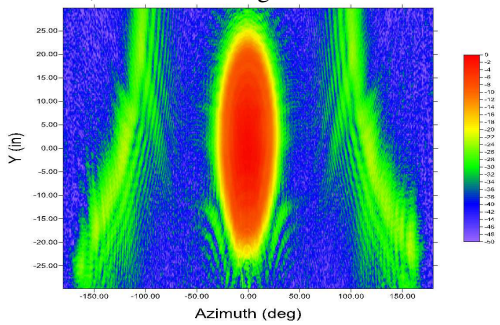

Figure 5. Full 360 degree cylindrical scan NF heat map.

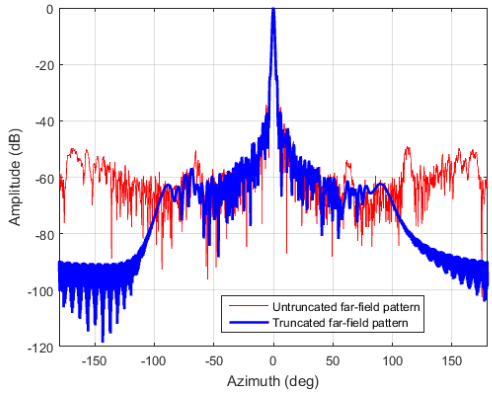

Figure 6. Far-field patterns of the co-pol component from truncated ($\phi=\pm 30^{o}$)- and full-aziumuthal NFs.

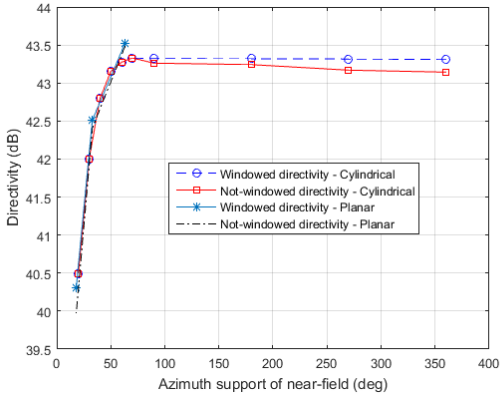

Figure 7. Windowed and standard (non-windowed) directivity for planar and cylindrical NF apertures, against azimuthal truncation.

As the truncation increases from the full 360° scan (seen by moving leftwards from the right hand side of the abscissa), the standard directivity increases gently, reaching a peak and coinciding with the windowed directivity for a truncation of 70°. The windowed directivity is constant through this range. Close to this truncation value, the planar aperture directivity is about a quarter of a dB higher than the cylindrical aperture directivity, and not affected by the far-field windowing. (The maximum planar aperture corresponds to a truncation of 63°) For further truncation, we are cutting into the high intensity zone of the heat map, and the directivity drops rapidly because of the decreased aperture size, but all four estimates are essentially the same in this range. The accuracy impact of the azimuth windowing is also in this graph. There is ~0.16dB difference between the windowed directivity and standard directivity, and this reduces to 0.032dB (regarded as negligible) for more truncation.

The planar aperture corresponds to 63° azimuth angle. Since the directivity difference is not affected as we truncate the scan size from 360° to 63°, the planar measurement can provide accurate enough directivity measurement compared with cylindrical which results in reducing the measurement time considerably. Of course we do not know if any of these values is the true directivity. The gain (or efficiency) is a much more difficult estimate, but its accuracy analysis must start with the directivity estimation accuracy.

5. Acknowledgements

Norsat International are thanked for providing the AUT.

6. References

1. A. D. Yaghjian, "An overview of near-field antenna measurements," *IEEE Transactions on Antennas and Propagation,* vol.34, no.1, pp. 30-45, 1986.
2. D. Slater, *Near-field antenna measurements*. Artech House, 1991, p. 247.
3. O. M. Bucci and M. D. Migliore, "A new method for avoiding the truncation error in near-field antennas measurements," *IEEE Transactions on Antennas and Propagation*, vol.54, no.10, pp. 2940-2952, Oct. 2006.
4. D. J. Van Rensburg, "Truncation study for design of a large spherical near-field antenna test system," *Proc. 16th IEEE International Symposium on Antenna Technology and Applied Electromagnetics (ANTEM)*, 2014.
5. C. Parini, D. J. Van Rensburg, S. Gregson, J. McCormick, *Theory and practice of modern antenna range measurements*. Electromagnetics and Radar Series, IET, vol. 55, 2014.
6. *NSI 2000 software*, Nearfield Systems Incorporated, NSI 2000, 1989.
7. A. Yaghjian, *Upper bound errors in far-field antenna parameter determined from planar near field measurements, Part 1: Analysis*, NBS Technical Note 667, US Department of Commerce/National Bureau of Standards, Oct. 1975.